



## Kinetics, thermodynamics and isotherm studies on adsorption of methyl orange from aqueous solution using ion exchange resin Amberlite IRA-400

Saroj Sekhar Behera<sup>a</sup>, Sourav Das<sup>b</sup>, Pankaj Kumar Parhi<sup>a,b,\*</sup>, Suraj Kumar Tripathy<sup>b</sup>, Ranjan Kumar Mohapatra<sup>c</sup>, Mayadhar Debata<sup>c</sup>

<sup>a</sup>School of Applied Sciences, School of Chemical Technology and Center of Industrial Technology, KIIT University, Bhubaneswar-751024, Odisha, India, Tel. +91-8280042882; emails: parhi\_pankaj@yahoo.co.in, parhipankaj@gmail.com (P.K. Parhi), sarosbehera@gmail.com (S.S. Behera)

<sup>b</sup>School of Biotechnology, School of Chemical Technology, and Center of Industrial Technology, KIIT University, Bhubaneswar-751024, Odisha, India, emails: sddassourav52@gmail.com (S. Das), tripathy.suraj@gmail.com (S.K. Tripathy)

<sup>c</sup>CSIR-Institute of Minerals and Materials Technology, Bhubaneswar-751013, Odisha, India, emails: mranjankumar.biotech@gmail.com (R.K. Mohapatra), mdebata@immt.res.in (M. Debata)

Received 8 February 2016; Accepted 8 July 2016

### ABSTRACT

Study on removal of anionic dye methyl orange (MO) from aqueous solution was investigated using ion exchange resin Amberlite IRA-400 batch adsorption process. Effect of operating adsorption factors that influence on the adsorption process such as contact time (1–300 min), initial dye concentration (25–500 ppm), solution pH (2.5–11.5), resin dose (5–100 g/L) and temperature (293–353 K) were studied. The extent of MO adsorption was increased with increase in the contact time, agitation speed, temperature, initial dye concentration and adsorbent dose but decreased with increase/decrease of the solution pH (maximum at pH-6.5). Equilibrium data were analyzed by both Langmuir isotherm and Freundlich adsorption isotherm. The maximum monolayer adsorption capacity of Amberlite IRA-400 was resulted as 74.4 mg/g at 303 K. The value of separation factor ( $R_L$ ) from Langmuir equation and Freundlich constant ( $n$ ) indicated on favorability of adsorption. Thermodynamic parameters such as  $\Delta G^\circ$ ,  $\Delta H^\circ$  and  $\Delta S^\circ$  were calculated and the positive value of  $\Delta H^\circ$  (4.13, 3.63 and 7.09 kJ mol<sup>-1</sup>) for corresponding initial MO dye concentrations: 50, 100 and 200 ppm, respectively, in the solution indicated that the adsorption was of endothermic in nature. Kinetics result revealed that the adsorption of MO is of pseudo second-order and chemisorptions type.

**Keywords:** Adsorption; Methyl orange (MO); Ion exchange; IRA 400; Kinetics

### 1. Introduction

Nowadays, organic contaminations from a various sources have become an important issue in worldwide because of their impact not only the public health but also the whole environment. Especially the organic dye pollutants from various industries like textile industry, paper, leather tanning, food processing, plastics, cosmetics, rubber, printing and dye manufacturing industries etc. have

received greater attention due to increasing of the environmental risk when they are discarded into water [1–6]. A very low concentrations of colored effluent though discharged into water bodies, that can again prevent the penetration of sunlight and oxygen throughout water as a result of which chemical and biochemical oxygen demands (COD and BOD) increases [4,7–9] and further it affect photosynthetic activity in aquatic systems [10–13]. However, some dyes are also degrading into various compounds which have toxic, mutagenic or carcinogenic influences on living organisms [5,10,11,14–17]. There are also some dyes which are resistant to aerobic digestion, and also stable to oxidizing agents

\* Corresponding author.

because of their synthetic processes and complex chemical structure which makes them exist in environment for a very long period of time [11,18]. Azo dye is one of them where the azo linkages ( $R_1-N=N-R_2$ ) shows various characteristics colors leading to their extensively usages in various industrial fields and also in research laboratories. However, when these azo dyes decomposed that produce at about 20 kinds of carcinogenic aromatic amines which can changes human DNA structure to result in induced lesions and cancer [5,6,19]. At present scenario more than 10,000 dyes are commercially available in worldwide and the production is approximately  $7 \times 10^5$  million tons. At about 5%–10% of these dyestuffs become waste which subsequently discharges into the aqueous phases as a result of which toxicity level of water bodies increases [4,11]. Of these dyes, sulpho-nated-based azo dye like MO is one of them, which is being most commonly used as an acid-base indicator. Therefore, it is very much essential to investigate the removal of azo dye from waste contaminated water due to this dye. Though preferentially preliminary pre-treatment of waste water is adopted while purifying waste water; there is still a big challenge prior to its disposal. This is mainly because synthetic dyes used in industries are designed to resist upon exposure to light, heat, many chemicals including oxidizing agents, water, sweat and microbial attacks [12,20].

In recent years, various techniques or methods are being practiced by the researchers for removal of dye from industrial effluents including photo catalytic degradation, sonochemical degradation, ozone treatment, micellar-enhanced ultra filtration, ion exchange membranes, electrochemical degradation, integrated chemical–biological degradation, integrated iron (III) photo-assisted biological treatment, solar photo-Fenton and biological processes and Fenton-biological treatment, coagulation and also adsorption [5,6,16,17,20–26]. Each of the above-mentioned methodology has some advantages and disadvantages. However, to overcome several issues such as incomplete removal of said metal/dye, usage of high cost reagent and high energy generation of toxic sludge or other waste products, high operating costs of these processes, an alternate effective method must be adopted. Adsorption is one of the most attracting technologies because of high efficient, cost-effective, simple design process, effortless operation in alternative to conventional methods as described above. The adsorption process is of eco-friendly approach because it does not produce any harmful substances after adsorption and on the other hand the availability of a wide range of adsorbents is high [27–30].

The adsorbent materials like activated carbons, modified clays, waste materials, zeolites, numerous bio-adsorbents were extensively being used in various adsorption processes [21,26,31,32]. However, the use of such adsorbent does not show greater potential in context of high selectivity and efficient removal of dyes or metal from the contaminated industrial waste water. Nevertheless, the above adsorbents have major drawback with regard to their regenerability issue. In contrast, commercially available polymeric resins such as Amberlite IR-120, Amberlite IR-400, Amberlite IRC-748, Amberlite IRC-718, and Lewatit TP-207 are found to be widely used in recent years as adsorbents due to good selectivity, binding energy and mechanical stability, easily regeneration property because

of bearing various specific functional (cationic/anionic/chelating exchange type) sites within it. Therefore, it can be used for multiple adsorption-desorption cycles and good reproducibility in sorption characteristics [16,32].

Wawrzkievicz [13] demonstrated that adsorptions of dyes using natural adsorbent are not more efficient as compared with synthesized product while investigating on comparative study of adsorption of C. I. Direct Blue 71 dye using different adsorbent (Amberlite IRA 67, Lewatit MonoPlus MP 62, Lewatit MonoPlus MP 64, Amberlite IRA 458, Amberlite IRA 900, Amberlite IRA 958, Lewatit MonoPlus MP 500, and Lewatit MonoPlus M 500) with natural sorbent materials such as orange peel. Both batch and column sorption methods were investigated for this adsorption process. Authors reported that the adsorbent material like Amberlite resin of IRA 958 (synthetic) was more efficient than the natural adsorbent material [13]. Karcher et al. [33] studied the effect of anion exchange resins S6328a (strong basic) and MP62 (weak basic) for removal of reactive dyes from textile wastewaters in which the regeneration of resin was easier in this process and the reaction was efficient when the pH of solution was below 8.0. Wawrzkievicz and Hubicki [34] also studied the effect of weak and strong base anion exchange resins (Amberlite IRA-67, Amberlite IRA-402, Amberlite IRA-958 and Lewatit M-600) for sorption of Indigo Carmine from aqueous solutions. From these results, the ion exchange capacities of Amberlite IRA-67, IRA-402, IRA-958 and Lewatit M-600 towards Indigo Carmine were 0.1 mmol/g, 0.17 mmol/g, 1.5 mmol/g and 0.21 mmol/g, respectively. They have also comparatively studied the potential adsorption of Acid Blue 29 using synthesized strongly basic anion exchange resin (Purolite A-520E) and natural adsorbent material of activated carbon (Purolite AC-20G), where Purolite A-520E showed high sorption capacity than activated carbon. Tang et al. [35] studied the removal of MO from aqueous solutions with poly (acrylic acid-co-acrylamide) superabsorbent resin and maximum of 394.6 mg/g loading efficiency was resulted at room temperature. Ma et al. [18] also studied the removal of MO and Methylene Blue from aqueous solution using alkali-activated multiwalled carbon nanotubes and in consequences, CNTs-A showed excellent adsorption capacity of 149 mg/g for MO and 400 mg/g for MB which can be attributed to multiple adsorption interaction mechanisms.

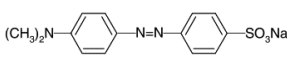
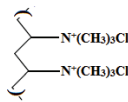
These results suggest that ion exchange resins in general could be effective sorbents for the removal of dyes from numerous industrial wastes or other aqueous medium. Nevertheless, the removal of MO using Amberlite IR-400 is scanty. Therefore, the objective of this work was to study on the removal of MO from the industrial waste water using anion exchanger resin Amberlite IRA-400. The sorption study on removal of MO by IRA 400 was investigated in the function of dye concentration, pH, shaking speed, contact time, temperature and resin dose rate. Langmuir and Freundlich isotherm models were derived from the results of initial dye concentration in the range 25–500 ppm study and reported. Further experimental data were analyzed to ensure the order of the adsorption reacting while fitting with the pseudo-first and pseudo-second-order intra particle diffusion model equations. Optimum experimental condition was established for quantitative removal of MO from waste water and the typical resin sample resulted was characterized by FT-IR, UV-VIS and described.

## 2. Experimental

### 2.1. Materials

Amberlite resin IRA-400 (average molecular weight is 341.917) was supplied from SD fine Chemical Ltd. The physical properties of the resin beads reported by suppliers are shown in Table 1. To ascertain the proposed adsorption mechanism, surface physical property characterization study of Amberlite IRA-400 resin was carried out by pore size analyzer, Pore master (Model no.: PM33GT-18, Quantachrome, USA, PVT LTD). The porosity characteristics such as pore diameter, pore volume, porosity and surface area of Amberlite IRA-400 resin was obtained as: 4.738053  $\mu\text{m}$ , 0.2824 cc/gm, 6.7246% and 3.03381  $\text{m}^2/\text{gm}$ , respectively. MO was procured from Himedia chemical reagent Ltd. The molecular structure and formula is also shown in Fig. 1. Sulphuric acid (Fisher Scientific), hydrochloric acid (Fisher Scientific), nitric acid (Fisher Scientific), sodium chloride (Merck), sodium hydroxide (Merck) used in this experiment were all of analytical grade.

Table 1  
General properties of MO dye and Amberlite IRA-400

Parameter	Remarks (MO dye)	Remarks (IRA-400)
Molecular formula	$\text{C}_{14}\text{H}_{14}\text{N}_3\text{NaO}_3\text{S}$	$\text{C}_{22}\text{H}_{28}\text{ClN}$
Molecular weight	327.33 g/mol	341.91
Structure		
Functional group	$\text{SO}_4^-$	$-\text{N}^+\text{R}_3$
Ionic form	$\text{Na}^+$	$\text{Cl}^-$

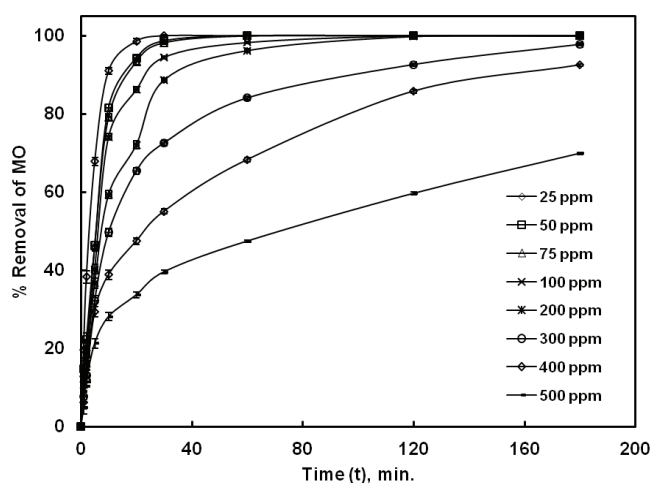


Fig. 1. Effect of initial dye concentration (conditions: 0.5 g of resin, temperature 303 K, pH 6.5, shaking speed 250 rpm).

### 2.2. Preparation and analysis of dye solution

For carrying out the adsorption study a stock solution of methyl orange (MO) dye of 1.0 g/l was prepared by dissolving the required amount of MO dye powder with distilled water. From that stock solution, the desired concentration of solution was prepared by diluting the stock solution. The desired concentration range of MO used in this investigation resembles to the concentration profile of industrial discharge waste effluent [2,5]. Estimation of MO was performed by colorimetric method and the absorbance of respective sample (s) was read at wavelength of 464 nm using a UV-Visible Spectrophotometer (UV-1800, Shimadzu, Japan). The pH of the aqueous samples were read using pH meter (Systronics model no. 361, India). Characterization of the MO loaded and original ion exchange resin bead Amberlite IRA-400 was performed by FTIR (in the region of 400–4,000  $\text{cm}^{-1}$ ) using SHIMAZDU, IRAffinity-1S FTIR Spectrophotometer, which further supported the above adsorption mechanism.

### 2.3. Experimental procedure

The adsorption experiments on Amberlite resin IRA-400 were carried out in batches. Adsorption on Amberlite resin of different dose were determined by performing adsorption tests in 250 ml Erlenmeyer flasks where 100 ml of MO solutions with different initial concentrations (25–500 ppm) were placed and put them on thermo-statted shaking incubator (LSI-3016R, Labtech, Korea). Adsorption experiments were carried out by varying pH, initial dye concentration, adsorbent dose, temperature and shaking speed. The temperature was controlled during the experiment to be  $\pm 1^\circ\text{C}$ . The pH of the solution was adjusted by adding 0.1 mol/L NaOH/HCl. The kinetics of the adsorption was carried out for a contact time range of 1–60 min, while keeping the resin amount constant in the shaking vessel. The adsorption isotherm was studied with a different initial mo dye concentration. The resin amount was varied from 0.1 to 5 g in the batch test adsorption study. The temperature of the solution was maintained at 303 K in most of the experiments except when the effect of temperature was studied in the range of 293–333 K. The shaking speed was kept fixed at 250 rpm in most of the batch test experiments except when the effect of agitation speed was studied in the range of 50–250 rpm. The amount of MO dye adsorbed by resin at equilibrium  $q_e$  ( $\text{mmol g}^{-1}$ ), and  $q_t$  ( $\text{mmol g}^{-1}$ ) at time “t” were obtained according to Eqs. (1) and (2), respectively, as follows:

$$q_e = \frac{(C_0 - C_e) \cdot V}{m} \quad (1)$$

$$q_t = \frac{(C_0 - C_t) \cdot V}{m} \quad (2)$$

In addition, the percentage of MO dye adsorbed from aqueous solution with the resin was calculated using Eq. (3):

$$\%M = \frac{(C_0 - C_t)}{C_0} \times 100 \quad (3)$$

where  $C_0$  and  $C_e$  ( $\text{mol.L}^{-1}$ ) are initial and equilibrium concentration of MO dye in aqueous phase, respectively,  $C_t$  ( $\text{mol.L}^{-1}$ )

is the concentration of MO at time  $t$ ;  $V$  (mL) is the volume of the solution and  $m$  (g) is the mass of dry resin. Other equations such as Eqs. (4)–(7) was fitted for interpreting the thermodynamics data, Eqs. (8)–(10) for fitting of kinetic modal and Eqs. (11)–(14) for fitting adsorption isotherm results and detail description for fitting of above equations are provided the respective sections. All the studies were executed by triplication of the experiments and, accordingly, the average of triplicate determinations data were reported. The standard deviations resulted in each experiments are provided in correspondence to the figures. Overall relative errors were obtained to be ~2.0%.

### 3. Results and discussions

#### 3.1. Effect of contact time and initial dye concentration

Effect of contact time for the study of adsorption of MO by Amberlite resin IRA 400 from 1–300 min was studied using 0.5 gm of resin in 100 ml of the aqueous solution while keeping other parameters fixed at: shaking speed 250 rpm, temperature 303 K, MO concentration range 25–500 ppm. It was seen from the results of Fig. 1 that the adsorption of MO increases from 14.99%–99.99%, 12.99%–99.99%, 10.99%–99.99%, 7.75%–97.94%, 6.05%–92.70% and 4.96%–70% with increase in the contact time from 1–60 min for 50 ppm, 1–120 min for 100 ppm and 1–180 min for 200, 300, 400 and 500 ppm, respectively, and thereafter, the adsorption efficiency remains unaltered up to 300 min [35]. The adsorption equilibrium of MO onto IRA-400 was attained at 60 min, 120 min and 180 min, respectively, for 50 ppm, 100 ppm and 200 ppm, indicating about requirement of higher contact time with corresponding higher initial MO concentration. The contact time of 60 min was kept fixed for further studies since studied initial concentration was of 50 PPM in most cases unless otherwise specified. Furthermore, the results of the adsorption of MO with three different initial concentrations (50, 100 and 200 ppm) at different time were interpreted (as discussed in kinetic model section) to obtain the order of the reaction.

Form this study, it was assured that the higher adsorption rate of MO was resulted within 30 min of contact time, though adsorption equilibrium was attained on 60 min and the observation for attaining rapid adsorption was attributed to the adequate free adsorptive site and high concentration gradient [5]. Similar to the results of the reported investigation [36,37], adsorption capacity of IRA 400 of present study showed that MO adsorption was increased with time in all studied initial concentration range and reached to a plateau value which revealed that the dye (MO) content is being adsorbed on to the resin site in of state of equilibrium with the amount of MO desorbed from the IRA 400. The adsorption rate was significantly enhanced while increasing the initial dye concentration (MO) of the solution and this may be due to strong interaction/exchange of anionic MO with IRA 400 [25].

#### 3.2. Effect of pH

The solution pH is most important factor in the adsorption process, since the variation of pH leads to the change in the degree of ionization of the MO dye and the surface properties

of adsorbent [38]. The effect of pH on removal of MO dye from aqueous solution at various solution pH (2.5–10.5) was shown in Fig. 2. From which, it can be seen that the maximum removal of dye was observed at pH 6.5 (merely neutral pH range). There was significant lowering of MO adsorption percentage was observed either by increasing pH beyond neutral pH range or by decreasing the pH below pH 6.5. The above observations can be explained by following reasons as: (i) at lower pH range, the  $H^+$  ion concentration increases and therefore, highly acidic medium of the solution prevents on strong ionization of  $SO_3^-$  of MO and that subsequently causes on lowering of MO adsorption. On the other hand, (ii) The loading of ionized form of MO ion on to IRA 400 resin phase was less pronounced due to increase in hydroxyl ion ( $OH^-$ ) at higher pH range (beyond neutral pH) [39]. This can further be explained due to the reason that the competitive effects of  $OH^-$  ion and the electrostatic repulsion between the anionic MO molecule and the negatively charged active adsorption site, i.e.,  $Cl^-$  of the IRA-400 is appears to be very high at alkaline pH ranges. The observations are in well agreement with the reported literature where the study MO adsorption was carried out using hydrothermal synthesized Mg-Al layered double hydroxide [36].

#### 3.3. Effect of shaking speed

The study of the effect of shaking speed on adsorption of dye was shown in Fig. 3. Adsorption is carried out by varying the shaking speed in the range of 50–250 rpm using 0.5 gm of resin dose with a solution of volume 100 ml, temperature 303 K and 50 ppm of MO concentration. As shown in Fig. 3, the percentage of MO adsorption increases with increase in the shaking speed. The adsorption of MO increases from 3.99% to 52.85%, 4.93% to 88.7%, 6.61% to 93.22%, 10.55% to 99.57% and 13.99% to 100% with the corresponding shaking speed of 50 rpm, 100 rpm, 150 rpm, 200 rpm and 250 rpm, respectively. From the results, it was ensured that % of MO removal beyond 200 rpm remained same and hence further experiments were carried out at 200 rpm shaking speed.

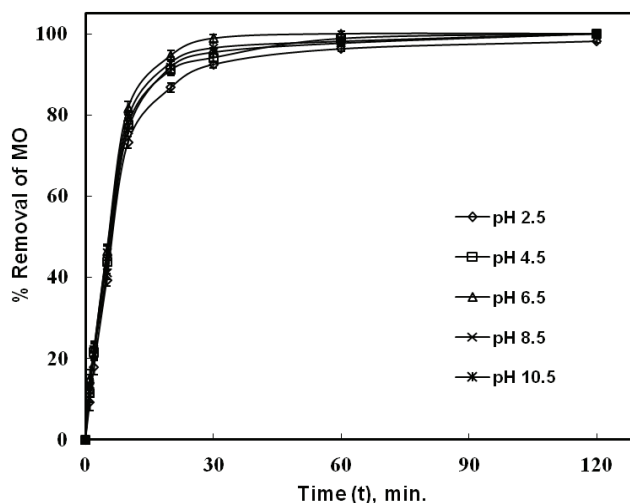


Fig. 2. Effect of pH on adsorption of MO (conditions: 0.5 g of resin, 50 ppm of dye, temperature 303 K, shaking speed 250 rpm).

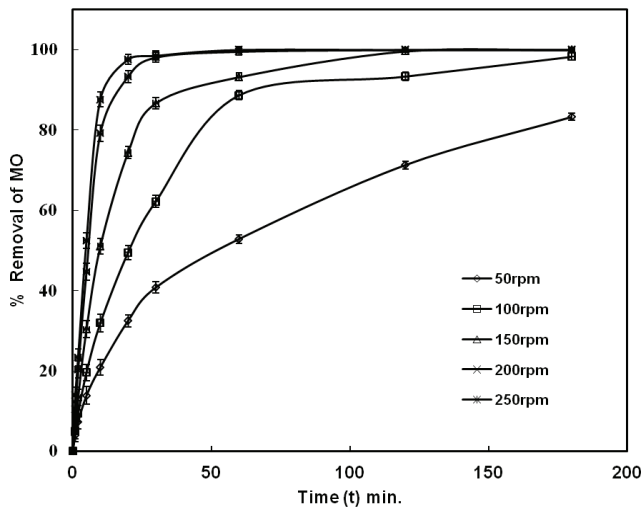


Fig. 3. Effect of shaking speed on adsorption of MO, conditions: mass of resin 0.5 gm, temperature 303 K, solution 100 ml.

The observation of achieving high adsorption efficiency may be due to mass transfer through pore diffusion unlike film diffusion which occurs at low agitation speed [40]. Thus, from this investigation, it was evident that at higher agitation speed, the film diffusion increases to a maximum value and pore diffusion thus becomes the rate controlling step and it was supported by the literatures [41].

### 3.4. Effect of adsorbent dosage

To find the optimum amount of adsorbent for maximum uptake of MO molecules by the adsorption sites of resin, study on variation of Amberlite IRA-400 quantity (0.1–5 g) was carried out while keeping rest of the parameters: pH 6.5, temp. 303 K time 180 min, shaking speed: 200 rpm, constant. The adsorption efficiency of MO was shown in Fig. 4. As can be seen from the results, the adsorption efficiency of MO showed increasing order from (29.64% to 99.99%) by increasing IRA-400 dosage in the range of 0.1–5 gm and adsorption equilibrium was achieved just after 10 min of contact time at higher resin dose (5 g) and on further increase in contact time and adsorbent site show only plateau. The enhancement of the adsorption efficiency at higher resin dose can be caused due to the increase in active sites of the resin which become available with the increase in mass of resin per unit volume solution [21].

### 3.5. Effect of temperature

It is well known that temperature has significant role during adsorption of dyes on to resin phase. Therefore, effect of temperature on the adsorption was investigated at varying range from 293–333 K. The results are shown in Fig. 5 and from which it was observed that while increasing the temperature of the solution the adsorption capacity of IRA 400 increases which favors about endothermic process (it was further interpreted with thermodynamic data resulted from the experiments as discussed below).

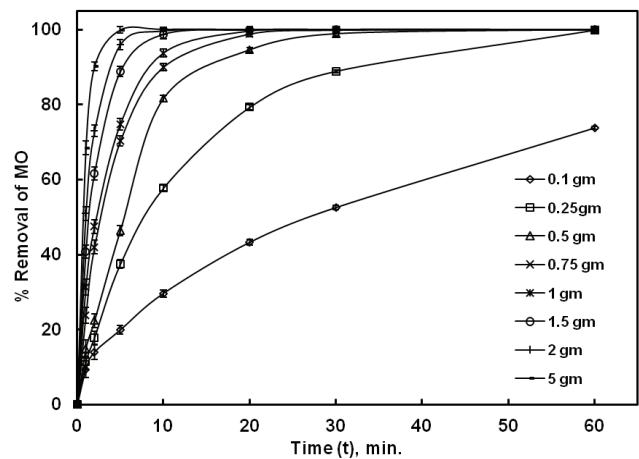


Fig. 4. Effect of adsorbent dose (conditions: shaking speed 250 rpm, 50 ppm of dye, temperature 303 K and pH 6.5).

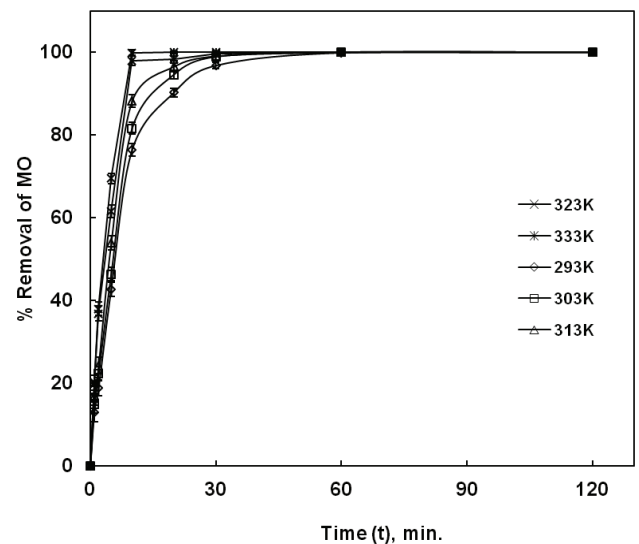


Fig. 5. Effect of temperature (conditions: 0.5 g of resin, 50 ppm, pH 6.5, shaking speed 250 rpm).

The equilibrium constant  $K_c$  for adsorption was calculated using the Eq. (4):

$$K_c = \frac{C_{Ae}}{C_e} \quad (4)$$

where  $C_{Ae}$  and  $C_e$  are the concentrations of MO in resin phase (g/L) and in solution (g/L) at equilibrium. Equilibrium loading capacity of dye was enhanced up to 0.431 mg/g, 0.44 mg/g, and 0.757 mg/g with corresponding initial dye concentration of 50 ppm, 100 ppm and 200 ppm, respectively, at temperatures ranges of 293 to 333 K. The values of  $\Delta G^\circ$ ,  $\Delta H^\circ$  and  $\Delta S^\circ$  can be calculated by following thermodynamic relationships in Eqs. (5)–(7).

$$\Delta G^\circ = -RT \ln K_c \quad (5)$$

$$\Delta G^\circ = \Delta H^\circ - T\Delta S^\circ \quad (6)$$

$$\log K_c = \frac{\Delta S^\circ}{2.303R} - \frac{\Delta H^\circ}{2.303RT} \quad (7)$$

where  $\Delta G^\circ$  is the standard free energy,  $\Delta H^\circ$  and  $\Delta S^\circ$  are the enthalpy and entropy change of adsorption process. The thermodynamic co-relation of rate constant  $K_c$  with standard free energy ( $\Delta G^\circ$ ) is described in Eqs. (5) and (6). The value of  $\Delta H^\circ$  and  $\Delta S^\circ$  were calculated from the slope and intercept, respectively, and presented in Table 2. The thermodynamics constants determined from the experimental study appear to be consistent and independent of initial dye concentration of the solution. The negative value of  $\Delta G^\circ$  indicated the feasibility of the adsorption process and the spontaneous interaction of MO dye ion with active sites of the resin. The positive values of  $\Delta H^\circ$  (+4.13, +3.63, +7.09) kJ mol<sup>-1</sup> corresponds to an endothermic nature of the adsorption process and the positive values of  $\Delta S^\circ$  (5.44, 4.11, 19.18) J mol<sup>-1</sup>K<sup>-1</sup> reveals the increased randomness of the dye and Amberlite resin IRA 400 interface during adsorption process. The increasing in adsorption efficiency of MO at higher temperature level may be caused due to increase rate of diffusion of the MO molecules across the external boundary layer and in the internal pores of the IRA-400 particles which subsequently leads to decrease the viscosity of the solution [2]. Moreover, the increase in temperature also shifts the equilibrium resin loading capacity from the bulk solution towards the IRA-400 surface and therefore, loading efficiency of resin to adsorb MO was significantly enhanced. On the other hand, the increase in temperature may result in the increase in activity of MO in solution as well as the strong affinity on exchanging the anionic site (Cl<sup>-</sup>) of IRA 400. The above reasons for high adsorption efficiency resulted at increased temperature level

Table 2  
Thermodynamic parameters of Amberlite IRA-400 adsorption at different initial MO dye concentration

Initial dye concentration (g/L)	Temperature, K	$\Delta G^\circ$ , kJ mol <sup>-1</sup>	$\Delta H^\circ$ , kJ mol <sup>-1</sup>	$\Delta S^\circ$ , J mol <sup>-1</sup> K <sup>-1</sup>
50 ppm	293	-2.52	4.13	5.44
	303	-2.50		
	313	-2.40		
	323	-2.36		
	333	-2.32		
100 ppm	293	-2.44	3.63	4.11
	303	-2.35		
	313	-2.31		
	323	-2.32		
	333	-2.27		
200 ppm	293	-1.56	7.09	19.18
	303	-1.12		
	313	-1.10		
	323	-0.85		
	333	-0.77		

of the present investigation are strongly supported by the reported literatures [10,26,42].

### 3.6. Kinetic model

The kinetic behaviors of the ion exchange resin IRA 400 with MO dye was examined in the systems with an initial dye concentration of 50 ppm. The pseudo-first-order kinetic model (30) described in Eq. (8) shown in Fig. 7 was fitted with the logarithmic form of the contact time data of Fig. 1. The rate constant of adsorption is determined from the first-order rate expression given by Lagergren and Svenska [20]:

$$\log(q_e - q_t) = \log q_e - \left(\frac{k_1}{2.303}\right) \cdot t \quad (8)$$

where  $q_e$  and  $q_t$  are the amounts of MO adsorbed (mg/g) at equilibrium and at time  $t$  (min), respectively, and  $k_1$  is the rate constant of adsorption (s<sup>-1</sup>).

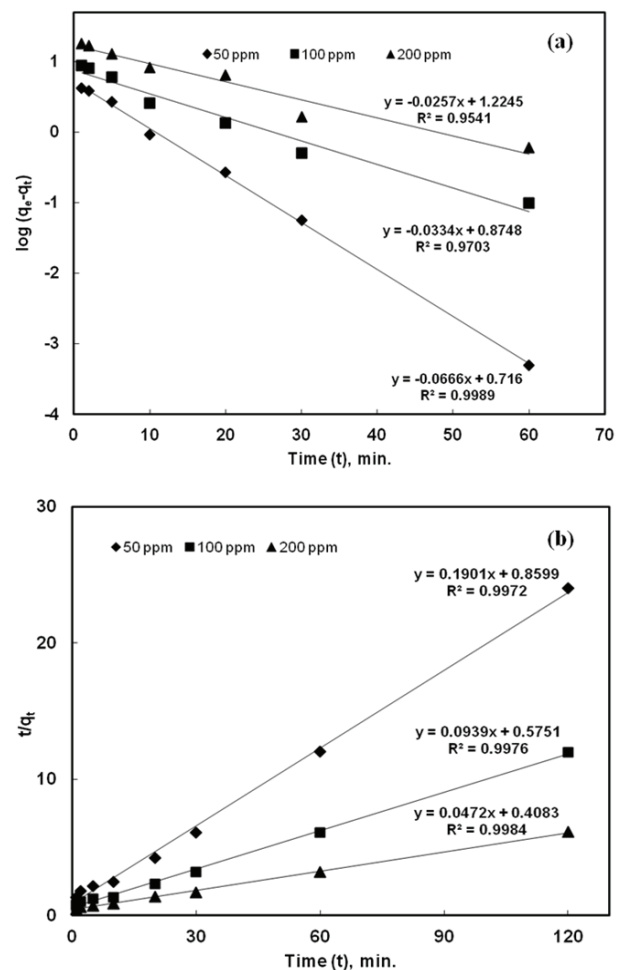


Fig. 6. (a) Pseudo-first-order kinetics for adsorption of MO by Amberlite IRA 400, (b) pseudo-second-order kinetics for adsorption of MO by Amberlite IRA 400, conditions: mass of resin 0.5 g, temperature 303 K, solution 100 ml.

The plot of  $\log(q_e - q_t)$  versus “ $t$ ” shown in Fig. 6(a) gives a straight line from which the rate constant  $k_1$  found from the slope value. The values of correlation coefficient  $R^2$ ,  $q_e$  and rate constant  $k_1$  are reported in Table 3. From this table, it was found that the values of  $q_e$  was significantly lower than the measured values, therefore, the rate of adsorption were further analyzed on the basis of the pseudo-second-order rate expression described in Eq. (9).

$$\frac{t}{q_t} = \frac{1}{k_2 q_e^2} + \frac{t}{q_e} \quad (9)$$

where  $k_2$  is the rate constant of the pseudo-second-order adsorption and the other terms have the same meaning as described in Eq. (9). The validity of second-order kinetics can be evaluated if the plot of  $t/q_t$  as the function of  $t$  (min) gives straight lines shown in Fig. 6(b). The values of slope ( $q_e$ ) intercept ( $k_2$ ) and correlation coefficient ( $R^2$ ) were calculated using the straight line of the graph and also listed in the Table 3. The calculated values of  $q_e$  from pseudo-second-order reaction are in reasonable agreement with the experimental  $q_e$  values from Fig. 6(b) listed in Table 3. From the above analytical data, it was presumed that the pseudo-second-order model provides better correlation of sorption fit than the pseudo-first-order model, suggesting that the rate limiting step may be of chemical sorption type [13,20]. The consistency of the resulted experimental data in this kinetics investigation study while fitting of the pseudo-second-order model ascertained the advantage for predicting the behavior over the whole ion exchange adsorption process. Moreover, it also indicates about the significance of the active sites found in the adsorbent matrix. Similar results are reported while removing the MO using different adsorbents in the literatures [21,25].

### 3.7. Mechanism of adsorption

The adsorption of MO from the synthetic waste solution using Amberlite resin IRA 400 appears to follow increasing trend with increase in the contact time and it was also

Table 3  
Kinetic parameters for MO adsorption with Amberlite IRA-400 at different initial concentrations

Initial MO dye concentration, mg/L	50	100	200
$q_e$ exp (mg/g)	4.99	9.99	19.98
Pseudo first order model			
$k_1$	0.1534	0.0769	0.0591
$q_e$ cal (mg/g)	5.2	7.5	16.8
$R^2$	0.9989	0.9703	0.9541
Pseudo-second-order model			
$k_2$	0.0414	0.0154	0.0055
$q_e$ cal (mg/g)	5.3	10.6	21.2
$R^2$	0.9972	0.9976	0.9986
Intra particle diffusion model			
$k_p$	1.2333	2.2773	3.5086
$R^2$	0.9564	0.9581	0.9513

observed that the adsorption process was very first at the initial period of contact time and then attained plateau with the increase in contact time. Therefore, the adsorption mechanism for the removal of dye can be explained by considering some assumptions [20] like:

- Migration of dye from the solution phase to the surface of the adsorbent material.
- Diffusion of dye through the boundary layer to the surface of the adsorbent.
- Adsorption of dye at an active site on the surface of adsorbent and also.
- Intra-particle diffusion of dye into the interior pores of the adsorbent particle.

The rate of adsorption process was mainly depends upon the resistance of boundary layer of the adsorbent molecule. With increase in the contact time, the resistance of the boundary layer decreases and leading to increase the mobility of the dye molecules. Thus, the rate of uptake of dye on the active sites of adsorbent mainly governed by either liquid phase mass transfer or diffusion through the boundary layer or intra-particle mass transfer.

Furthermore, the adsorption process will not only occur at the external surface of the resin but also may diffuse into the inner layer of the porous resin. That intra-particle diffusion can be explained using the intra-particle diffusion model of Weber-Morris [12] on the rate of MO dye adsorption with Amberlite Resin IRA 400, described by Eq. (10):

$$q_t = X_i + k_p t^{1/2} \quad (10)$$

where  $q_t$  is the concentration of MO dye adsorbed at a given time  $t$  (min),  $k_p$  ( $\text{mg/g} \cdot \text{min}^{0.5}$ ) is the intra particle diffusion rate constant and  $X_i$  is the intercept, for which the effect of the intra particle diffusion model for our experiment was studied, where the linearity behavior of MO adsorption profile indicated the control of adsorption by intra particle diffusion of the MO dye within the pores of resin to the adsorption sites. From the slope of the plot the  $k_p$  values was calculated and shown in Table 3. The above adsorption mechanism can also be studied by UV-VIS characterization where the study of MO before and after adsorption with IRA-400 was performed within the range of 200–800 nm and the results are

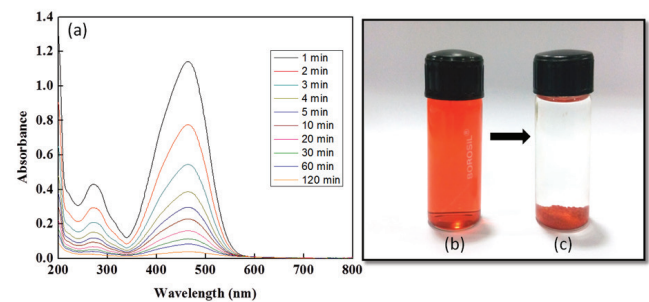


Fig. 7. (a) UV-Visible spectral analysis results on adsorption of MO by Amberlite IRA 400 Ion-exchange resin and a view of adsorption process, (b) MO dye solution before adsorption, (c) after adsorption of MO by IRA 400 resin beads.

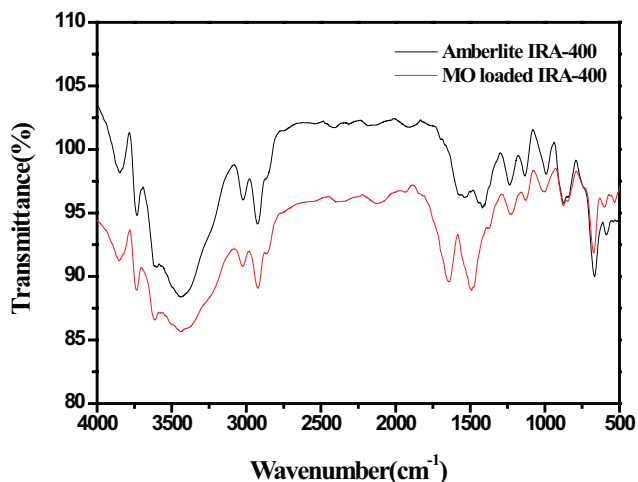


Fig. 8. FTIR of Amberlite IRA-400 and MO loaded IRA-400.

shown in Fig. 7(a). The characteristics absorption peaks at different time of aqueous MO bearing samples after adsorption revealed about decreasing MO concentration profile with increasing in adsorption time length [43]. This was further evident from Fig. 7(b) due to degradation of MO color after adsorption and the appearance of the orange color in the MO-loaded resin phase was due to the adsorption of MO on to the resin IRA 400 phase.

FTIR spectrum of Amberlite resin IRA-400 before adsorption and after MO dye adsorption was shown in Fig. 8. This showed various absorption bands for corresponding various functional group which is responsible for binding of dye molecule. The band observed at 1,003 and 1,134  $\text{cm}^{-1}$  correspond to  $\nu(\text{S}=\text{O})$  of the  $-\text{SO}_3^-$  group in the loaded IRA-400 was found in MO-loaded resin phase that may be due to the presence of above functional group of MO in the resin bead surface [18]. The absorption peak 1,485 and 1,642  $\text{cm}^{-1}$  due to  $\nu(\text{N}=\text{N})$  and aromatic ring of MO, respectively, was appeared in MO loaded functionalized resin. This confirms the association of MO with Amberlite IRA-400(Cl<sup>-</sup>) [44]. The band appearing at 2,950  $\text{cm}^{-1}$  is due to the  $\nu(\text{C}-\text{H})$  of  $\text{CH}_3$  found in both the cases. The band appears at 1,240  $\text{cm}^{-1}$  corresponds to  $\nu(\text{C}-\text{N})$  was also found in both original IRA 400 as well as loaded resin phase. Based on the FTIR results the functional group characteristics property was ensured. In addition, the Boehm titration method was further adopted while taking equal concentration of  $\text{NaOH}$ ,  $\text{Na}_2\text{CO}_3$  and  $\text{NaHCO}_3$  and  $\text{HCl}$  [45]. From the results, it was assured that the exchanging site was basic in nature having tertiary ammonium chloride form. Based on the FTIR study and Boehm titration results possible, the adsorption/ion exchange mechanism of MO with Amberlite IRA 400 was proposed as presented in Fig. 9. There is the exchange of the anionic MO species with chloride ion of IRA 400 [46].

### 3.8. Adsorption isotherms

To establish the mechanism of MO adsorption on the Amberlite Resin 400 at different initial MO concentration (from 0.05 to 0.5 g/L) the experimental data were applied to the Langmuir and Freundlich isotherm equations, where

other parameters were as follows: resin mass of 0.5 gm, agitation speed 250 rpm, pH 6.5, temp 303 K and solution volume of 100 ml. As shown in Fig. 1, it was seen that the amount of MO dye adsorbed per unit mass of resin increased with time and reached the plateau value when the active sites of the resin bed were saturated. The equilibrium adsorption data of different initial dye concentrations listed in Table 4 were analyzed according to Langmuir and Freundlich adsorption isotherm models [5,13] as given in Eqs. (11) and (12), respectively.

$$\frac{C_e}{q_e} = \frac{1}{bq_m} + C_e \left( \frac{1}{q_m} \right) \quad (11)$$

$$\log q_e = \log K_F + \frac{1}{n} \log C_e \quad (12)$$

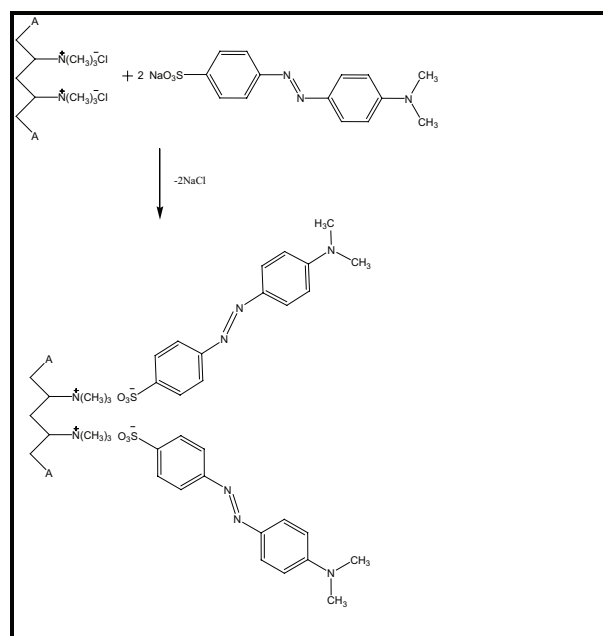


Fig. 9. Adsorption mechanism of MO with Amberlite IRA 400 resin.

Table 4  
Equilibrium adsorption results of MO dye at different initial concentration

Initial MO dye concentration, mg/L	Equilibrium concentrations, mg/L (303 K)	
	$C_e$	$q_e$
25	4.99	2.499
50	9.98	4.999
75	14.99	7.499
100	19.97	9.989
200	39.99	19.95
300	59.95	29.97
400	93.11	46.55
500	70.23	35.11



where  $q_e$  is the amount of dye adsorbed at the equilibrium (mg/g),  $C_e$  is the concentration of solution at the equilibrium state of the system (ppm),  $b$  is the Langmuir constant (L/mg), and  $q_m$  is the maximum adsorption capacity (74.4 mg/g) and  $K_F$  is the Freundlich constant (L/mg). From Langmuir adsorption isotherm model, the values of  $R^2$ ,  $q_m$  and  $b$  were determined from the slope and intercept of the straight line of a plot of  $C_e/q_e$  vs.  $C_e$  shown in Fig. 10(a) and results are given in Table 5. From the Fig. 10(a), the correlation coefficient ( $R^2$ ) was found to be well fitted to the experimental data in case of Langmuir isotherm's model (Table 5). It also suggests that all of the adsorption sites are of equivalent energy.

Table 5  
Langmuir and Freundlich isotherm parameters for MO dye adsorption with Amberlite resin of IRA-400 at 303 K temperature

Temp. K	Langmuir isotherm			Freundlich isotherm		
	$q_m$ , mmol.g <sup>-1</sup>	$b$ , mmol <sup>-1</sup>	$R^2$	$n$	$k_F$	$R^2$
303	5,000	0.0001	0.9998	0.995	2.007	0.998

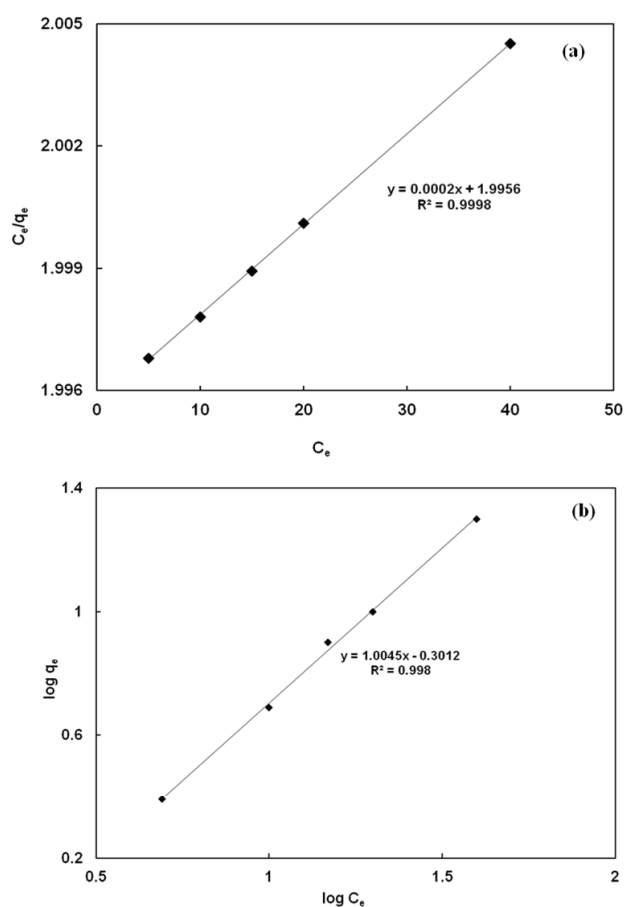


Fig. 10. (a) Plot of Langmuir isotherm for adsorption of MO by Amberlite IRA 400, (b) plot of Freundlich isotherm for adsorption of MO by Amberlite IRA 400. Conditions: mass of resin 0.5 g, temperature 303 K, solution 100 ml.

The essential characteristic of the Langmuir isotherm can be expressed by the dimensionless constant called equilibrium parameter,  $R_L$ , defined by:

$$R_L = 1 / (1 + bC_0) \quad (13)$$

where  $b$  is the Langmuir constant and  $C_0$  is the highest initial dye concentration. From this  $R_L$  we can determine the process of adsorption isotherm. The adsorption isotherm is irreversible if  $R_L = 0$ , the isotherm is favorable if  $0 < R_L < 1$ , linear if  $R_L = 1$  or unfavorable if  $R_L > 1$ . The  $R_L$  values for the adsorption of MO dye on the resin sample were calculated and were found to be 0.0739, 0.0383, 0.0259, 0.0195, 0.0098, 0.0066, 0.0049 and 0.0039 for the MO dye concentration of 25 ppm, 50 ppm, 75 ppm, 100 ppm, 200 ppm, 300 ppm, 400 ppm and 500 ppm, respectively, at temperature 303 K, indicating that the adsorption of MO on resin is favorable [10,13,23,30].

The adsorption data were further interpreted while fitting with Freundlich isotherm model. The plots of  $\log q_e$  vs.  $\log C_e$  also showed straight lines in Fig. 10(b). As it is known that the value of  $K_F$  indicates about adsorption capacity and  $1/n$  is the adsorption intensity and both of these values can be derived from the slope of the above plot. The values of  $R^2$ ,  $K_F$  and  $1/n$  obtained from the slope and intercept of the straight line are also listed in Table 5, where  $q_e$  represents the quantity of dye adsorbed onto adsorbent at unit equilibrium concentration and  $n$  represents the degree of favorability of adsorption. In general, the value of  $n$  found to be less than 10 and higher than unity that reveals on favoring for adsorption condition and in this study the value was obtained as 0.995, which is slightly close than unity; therefore, overall results do not fit well as compared with Langmuir Isotherm. Nonetheless, while comparing the results of Freundlich with Langmuir isotherm model, Langmuir Isotherm showed better fit as  $R^2$  values is very close to unity. The best fit of equilibrium data in the Langmuir isotherm ensures the monolayer coverage of MO onto IRA400 resin beads [47].

### 3.9. Elution study

To study the elution of dye (MO), the MO-loaded Amberlite resin phase (adsorbed at pH 6.5 for 60 min) was treated different acid, alkali and salt reagents ( $\text{NH}_4\text{OH}$ , HCl,  $\text{NH}_4\text{Cl}$ ,  $\text{H}_2\text{SO}_4$ ,  $\text{HNO}_3$ , NaCl). As can be seen from the results of Fig. 11, the percentage of desorption of MO was less pronounced with alkaline reagents or salts. However, desorption was significantly high with acidic reagents (HCl,  $\text{H}_2\text{SO}_4$ ,  $\text{HNO}_3$ ), which was well evident from the initial reagent screening study. Of these, maximum desorption of 99.7% was found with both HCl solution and the elution efficiency of above reagents follows the order as  $\text{HCl} > \text{H}_2\text{SO}_4 > \text{HNO}_3 > \text{NaCl} > \text{NH}_4\text{Cl} > \text{NH}_4\text{OH}$ . Therefore, further desorption of MO from MO loaded resin IRA-400 while varying acid concentration was studied using HCl solution and the results were as shown in Fig. 12, from which it was found that the desorption of MO increased from 40.55% to 99.71% with increase in HCl concentration from 0.1 to 1.0 M, respectively, after 3 h of contact time at 303 K and it was insignificant on further increase in time (up to 5 h). Moreover, the desorption efficiency of MO from MO-Loaded resin phase observed to be increases with time at the studied HCl concentration level,

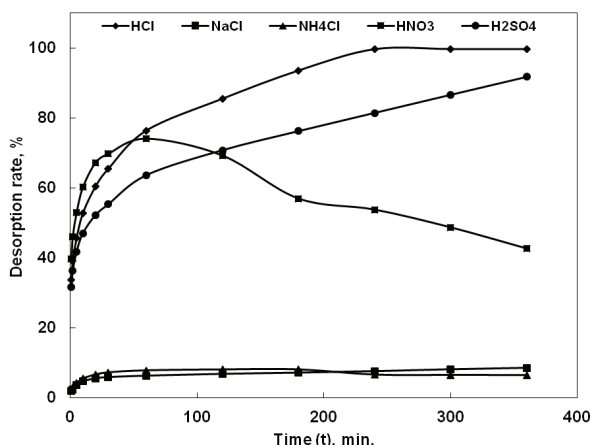


Fig. 11. Plot of desorption efficiency of MO dye from MO-loaded Amberlite resin IRA 400 using various solvent. Conditions: agitation speed of 250 rpm, temperature 303 K.

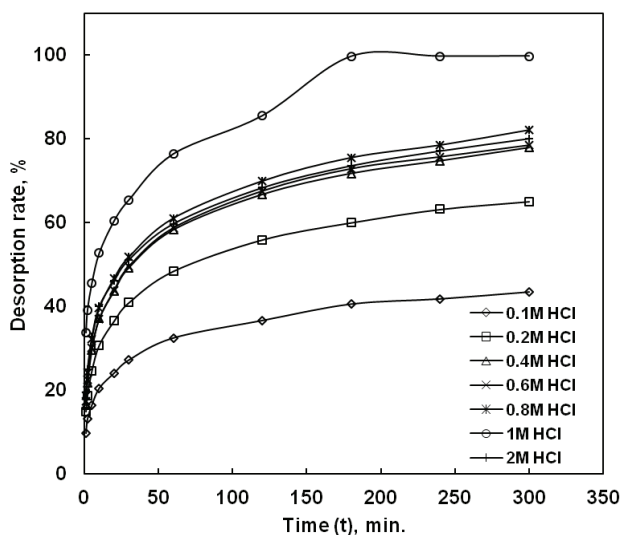


Fig. 12. Effect of desorption efficiency of MO dye from MO-loaded Amberlite resin IRA 400. Conditions: agitation speed of 250 rpm, temperature 303 K.

though, it was maximized with 1.0 M HCl. Hence, 1.0 M HCl will be sufficient for quantitative desorption of MO from MO-loaded IRA 400 phase vis-a-vis more than 99% yield on regeneration of IRA 400 after 3 h of contact time at ambient temperature condition.

#### 4. Conclusion

Removal of MO from the aqueous solution bearing 50 ppm using anion exchange resin IRA400 was investigated. The adsorption studies were carried out as a function of contact time, temperature, resin dose, initial dye concentration and pH of the solution. The resulted data of the above adsorption parameters was rigorously interpreted by Kinetics, thermodynamic and isotherm study to establish the mechanism of adsorption process of MO onto

IRA400 beads. The adsorption of MO with resin was critical with the influence of time, temperature and pH. Percentage removal of the dye was decreased with increase in initial dye concentration, whereas increased with increase time, temperature and adsorption equilibrium was achieved in just after 60 min of the treatment. pH affects the surface charge of the adsorbent and the degree of ionization of adsorbate and adsorption was efficient at merely neutral water pH range (pH-6.5). The adsorption of MO was also enhanced while increasing resin dose as well as initial MO concentration. Maximum loading capacity of MO was obtained to be 74.4 mg/g by IRA-400 in this study which seems significantly larger than the reported literatures. Experimental equilibrium data showed best fit with the Langmuir isotherm model as compared with the Freundlich isotherm though  $R^2$  values of both were close to unity, indicating monolayer sorption on a homogeneous surface. The monolayer sorption capacity increased with increase in temperature from 298 K to 333 K. Thermodynamic parameters such as change in Gibbs free energy ( $\Delta G^\circ$ ), adsorption enthalpy ( $\Delta H^\circ$ ) and adsorption entropy ( $\Delta S^\circ$ ) were determined showed the relevance on favoring the adsorption process. The positive value of  $\Delta S^\circ$  suggesting an increase in degrees of freedom of adsorbed species and positive value of  $\Delta H^\circ$  indicated that the process is of endothermic in nature. The present investigation ensured that IR400 can be an effective anion exchanger while applying on purification of contaminated water/process aqueous solution at the neutral pH range. Elution of MO using 1 M HCl was adequate enough to regenerate at about 99% of Amberlite IRA-400 after 3 h of contact time.

#### Acknowledgements

Authors P.K. Parhi and S. Tripathy are highly grateful and would like to acknowledge Department of Science and Technology (DST), New Delhi, Govt. of India for the financial assistance and support provided under DST-INSPIRE Faculty scheme (DST/IFA/CH-26/2012). Author P.K. Parhi also would like to acknowledge SERB, DST, New Delhi, Govt. of India for providing partial financial support under young scientist award (start-up research grant) scheme (SB/FT/CS-076-2014) for the investigation of this work. Co-authors S.S. Behera and S. Das also wish to acknowledge DST, New Delhi, Govt. of India, for partially funding the work.

#### References

- [1] M.T. Yagub, T.S. Sen, S. Afroz, H.M. Ang, Dye and its removal from aqueous solution by adsorption: a review, *Adv. Colloid. Interface Sci.*, 209 (2014) 172–184.
- [2] R.D.C. Soltani, A.R. Khataee, M. Safari, S.W. Joo, Preparation of bio-silica/chitosan nanocomposite for adsorption of a textile dye in aqueous solutions, *Int. Biodeterior. Biodegradation*, 85 (2013) 383–391.
- [3] S. Elemen, E.P.A. Kumbasar, S. Yapar, Modelling the adsorption of textile dye on organoclay using an artificial neural network, *Dyes Pigments*, 95 (2012) 102–111.
- [4] S. Liu, Y. Ding, P. Li, K. Diao, X. Tan, F. Lei, Y. Zhan, Q. Li, B. Huang, Z. Huang, Adsorption of the anionic dye Congo red from aqueous solution onto natural zeolites modified with N,N-dimethyl dehydroabietylamine oxide, *Chem. Eng. J.*, 248 (2014) 135–144.

- [5] J. Zhang, Q. Zhou, L. Ou, Kinetic, isotherm, and thermodynamic studies of the adsorption of methyl orange from aqueous solution by chitosan/alumina composite, *J. Chem. Eng. Data.*, 57 (2012) 412–419.
- [6] Y. Fan, H.J. Liu, Y. Zhang, Y. Chen, Adsorption of anionic MO or cationic MB from MO/MB mixture using polyacrylonitrile fiber hydrothermally treated with hyper branched polyethylenimine, *J. Hazard. Mater.*, 283 (2015) 321–328.
- [7] V. Nair, A. Panigrahy, R. Vinu, Development of novel chitosan-lignin composites for adsorption of dyes and metal ions from wastewater, *Chem. Eng. J.*, 254 (2014) 491–502.
- [8] Q. Peng, M. Liu, J. Zheng, C. Zhou, Adsorption of dyes in aqueous solutions by chitosanhalloysite nanotubes composite hydrogel beads, *Microporous Mesoporous Mater.*, 201 (2015) 190–201.
- [9] M.S. Derakhshan, O.J. Moradi, The study of thermodynamics and kinetics methyl orange and malachite green by SWCNTs, SWCNT-COOH and SWCNT-NH<sub>2</sub> as adsorbents from aqueous solution, *Ind. Eng. Chem.*, 20 (2014) 3086–3094.
- [10] A.A. Jalil, S. Triwahyono, S.H. Adam, N.D. Rahim, M.A.A. Aziz, N.H.H. Hairom, A.N.M. Razali, M.A.Z. Abidin, M.K.A. Mohamadiaha, Adsorption of methyl orange from aqueous solution onto calcined Lapindo volcanic mud, *J. Hazard. Mater.*, 181 (2010) 755–762.
- [11] D. Elhamifar, F. Shojaeipoor, M. Roosta, Self-assembled ionic-liquid based organosilica (SAILBO) as a novel and powerful adsorbent for removal of malachite green from aqueous solution, *J. Taiwan. Inst. Chem. Eng.*, 59 (2016) 267–274.
- [12] P. Monvisade, P. Siriphannon, Chitosan intercalated montmorillonite: preparation, characterization and cationic dye adsorption, *Applied. Clay. Sci.*, 42 (2009) 427–431.
- [13] M. Wawrzekiewicz, Anion-exchange resins for C.I. Direct Blue 71 removal from aqueous solutions and wastewaters: effects of basicity and matrix composition and structure, *Ind. Eng. Chem. Res.*, 53 (2014) 11838–11849.
- [14] D. Ljubas, G. Smoljanic, H. Juretic, Degradation of methyl orange and Congo Red dyes by using TiO<sub>2</sub> nanoparticles activated by the solar and the solar-like radiation, *J. Environ. Manage.*, 161 (2015) 83–91.
- [15] L. Ai, C. Zhang, L. Meng, Adsorption of methyl orange from aqueous solution on hydrothermal synthesized Mg-Al layered double hydroxide, *J. Chem. Eng. Data.*, 56 (2011) 4217–4225.
- [16] S.G. Muntean, M.E. Radulescu-Grad, P. Sfarloag, Dye adsorbed on copolymer, possible specific sorbent for metal ions removal, *RSC Adv.*, 4 (2014) 27354–27362.
- [17] G. Sheng, A. Alsaedi, W. Shammakh, S. Monaquel, J. Sheng, X. Wang, H. Li, Y. Huang, Enhanced sequestration of selenite in water by nanoscale zero valent iron immobilization on carbon nanotubes by a combined batch, XPS and XAFS investigation, *Carbon*, 99 (2016) 123–130.
- [18] J. Ma, F. Yu, L. Zhou, L. Jin, M. Yang, J. Luan, Y. Tang, H. Fan, Z. Yuan, J. Chen Enhanced adsorptive removal of methyl orange and Methylene Blue from aqueous solution by alkali-activated multiwalled carbon nanotubes, *Appl. Mater. Interfaces.*, 4 (2012) 5749–5760.
- [19] H.Y. Zhua, R. Jiang, L. Xiao, W. Li, A novel magnetically separable Fe<sub>2</sub>O<sub>3</sub>/crosslinked chitosan adsorbent: preparation, characterization and adsorption application for removal of hazardous azo dye, *J. Hazard. Mater.*, 179 (2010) 251–257.
- [20] S. Karaca, A. Gurses, O. Acisli, A. Hassania, M. Kiransan, K. Yikilmaz, Modeling of adsorption isotherms and kinetics of Remazol Red RB adsorption from aqueous solution by modified clay, *Desal. Wat. Treat.*, 51 (2013) 2726–2739.
- [21] M. Arshadi, F. SalimiVahid, J.W.L. Salvacion, M. Soleymanzadeh, Adsorption studies of methyl orange on an immobilized Mn-nanoparticle: kinetic and thermodynamic, *RSC Adv.*, 4 (2014) 16005–16017.
- [22] M.Z. Iqbal, A.A. Abdala, Thermally reduced graphene: synthesis, characterization and dye removal applications, *RSC Adv.*, 3 (2013) 24455–24464.
- [23] G. Sheng, J. Hu, H. Li, J. Li, Y. Huang, Enhanced sequestration of Cr(VI) by nanoscale zero-valent iron supported on layered double hydroxide by batch and XAFS study, *Chemosphere*, 148 (2016) 227–232.
- [24] R. Rakhshae, M. Gahi, A. Pourahmad, Removal of methyl orange from aqueous solution by Azolla filiculoides: synthesis of Fe<sub>3</sub>O<sub>4</sub> nano-particles and its surface modification by the extracted pectin of Azolla, *Chinese. Chem. Lett.*, 22 (2011) 501–504.
- [25] W. Cheah, S. Hosseini, M.A. Khan, T.G. Chuah, T.S.Y. Choong, Acid modified carbon coated monolith for methyl orange adsorption, *Chem. Eng. J.*, 215–216 (2013) 747.
- [26] M. Arshadia, F.V. Salimi, J.W.L. Salvacion, M. Soleymanzadeh, A practical organometallic decorated nano-size SiO<sub>2</sub>-Al<sub>2</sub>O<sub>3</sub> mixed-oxides for methyl orange removal from aqueous solution, *Appl. Surf. Sci.*, 280 (2013) 726–736.
- [27] P. Tian, X.Y. Han, G.L. Ning, H.X. Fang, J.W. Ye, W.T. Gong, Y. Lin, Synthesis of porous hierarchical MgO and its superb adsorption properties, *ACS Appl. Mater. Interfaces.*, 5 (2013) 12411–12418.
- [28] R. Gong, J. Ye, W. Dai, X. Yan, J. Hu, X. Hu, S. Li, H. Huang, Adsorptive removal of methyl orange and Methylene Blue from aqueous solution with finger citron residue-based activated carbon, *Ind. Eng. Chem. Res.*, 52 (2013) 14297–14303.
- [29] B. Tanhaei, A. Ayati, M. Lahtinen, M. Sillanpaa, Preparation and characterization of a novel chitosan/Al<sub>2</sub>O<sub>3</sub>/magnetite nanoparticles composite adsorbent for kinetic, thermodynamic and isotherm studies of methyl orange adsorption, *Chem. Eng. J.*, 259 (2015) 1–10.
- [30] Y. Yao, B. He, F. Xu, X. Chen, Equilibrium and kinetic studies of methyl orange adsorption on multiwalled carbon nanotubes, *Chem. Eng. J.*, 170 (2011) 82–89.
- [31] M. Greluk, Z. Hubicki, Efficient removal of Acid Orange 7 dye from water using the strongly basic anion exchange resin Amberlite IRA-958, *Desalination*, 278 (2011) 219–226.
- [32] C. Karthika, M. Sekar, Removal of Hg (II) ions from aqueous solution by acid acrylic resin: a study through adsorption isotherms analysis, *J. Environ. Sci.*, 1 (2012) 34–41.
- [33] S. Karcher, A. Kormmuller, M. Jekel, Anion exchange resins for removal of reactive dyes from textile wastewaters, *Water Res.*, 36 (2002) 4717–4724.
- [34] M. Wawrzekiewicz, Z. Hubicki, Equilibrium and kinetic studies on the sorption of acidic dye by macroporous anion exchanger, *Chem. Eng. J.*, 157 (2010) 29–34.
- [35] Y. Tang, X. Wang, L. Zhu, Removal of methyl orange from aqueous solutions with poly(acrylic acid-co-acrylamide) superabsorbent resin, *Polym. Bull.*, 70 (2013) 905–918.
- [36] L. Ai, C. Zhang, L. Meng, Adsorption of methyl orange from aqueous solution on hydrothermal synthesized Mg-Al layered double hydroxide, *J. Chem. Eng. Data*, 56 (2011) 4217–4225.
- [37] S. Hosseini, M.A. Khan, M.R. Malekbala, W. Cheah, T.S.Y. Choong, Carbon coated monolith, a mesoporous material for the removal of methyl orange from aqueous phase: adsorption and desorption studies, *Chem. Eng. J.*, 171 (2011) 1124–1131.
- [38] L. Zhou, J. Jin, Z. Liu, X. Liang, C. Shang, Adsorption of acid dyes from aqueous solutions by the ethylenediamine-modified magnetic chitosan nanoparticles, *J. Hazard. Mater.*, 185 (2011) 1045–1052.
- [39] M.A. Khan, Z.A.A. Othman, M. Kumar, M.S. Ola, M.R. Siddique, Biosorption potential assessment of modified pistachio shell waste for methylene blue: thermodynamics and kinetics study, *Desal. Wat. Treat.*, 56 (2014) 1–15.
- [40] S.D. Khattri, M.K. Singh, Removal of malachite green from dye wastewater using neem sawdust by adsorption, *J. Hazard. Mater.*, 167 (2009) 1089–1094.
- [41] B. Nandi, A. Goswami, M. Purkait, Removal of cationic dyes from aqueous solutions by kaolin: kinetic and equilibrium studies, *Appl. Clay. Sci.*, 42 (2009) 583–590.
- [42] G. Sheng, H. Dong, Y. Li, Characterization of diatomite and its application for the retention of radiocobalt: role of environmental parameters, *J. Environ. Radioact.*, 113 (2012) 108–115.
- [43] T.T. Ali, K. Narasimharao, I.P. Parkin, C.J. Carmalt, S. Sathasivam, S.N. Basahel, S.M. Bawaked, S.A. Al-Thabiti, Effect of pretreatment temperature on photo catalytic activity of microwave irradiated porous nanocrystalline ZnO, *New J. Chem.*, 39 (2015) 321–332.

- [44] K.H. Park, P.K. Parhi, N.H. Kang, Studies on removal of low content copper from the sea nodule aqueous solution using the cationic resin TP 207, *Separ. Sci. Technol.*, 47 (2012) 1531–1541.
- [45] I.I. Salame, T.J. Bandosz, Surface chemistry of activated carbons: combining the results of temperature-programmed desorption, Boehm, and potentiometric titrations, *J. Colloid. Interf. Sci.*, 240 (2001) 252–258.
- [46] R. Bahadur, Removal of Pb(ii) ion by using modified anion ion exchanger, Amberlite IRA-400, *J. Environ. Res. Develop.*, 9 (2015) 744–754.
- [47] H. Li, Z. Sun, L. Zhang, Y. Tian, G. Cui, S. Yan, A cost-effective porous carbon derived from pomelo peel for the removal of methyl orange from aqueous solution, *Colloid. Surface. A.*, 489 (2016) 191–199.